α^2 CVn: A comparison between Spot and Oblate Spheroid Models

Praveen Nagar & K. D. Abhyankar *Department of Astronomy, Osmania University, Hyderabad 500007*

Abstract. A comparison is made between a hot-spot model and a recently proposed oblate spheroid model (Böhm-Vitense & Van Dyk 1987) to explain the spectroscopic and photometric variations of α^2 CVn. It is found that the spot model gives a better fit to the spectroscopic and photometric variations. The spot model requires five high temperature circular patches over the surface of the star. The positions of these patches agree well with those derived spectroscopically by Pyper (1969).

Key words: stars—Ap stars—spot modelling

1. Introduction

Among all the Ap stars, α^2 CVn is the brightest ($m_v = 2.9$) and one of the most observed peculiar stars. Its photometric variability was first reported by Guthnick & Prager (1914). α^2 CVn also shows a variable spectrum and a variable magnetic field. An extensive study of this star was carried out by Pyper (1969). Pyper found the equivalent width of rare-earth lines varying with a period of 5.5 days. Its light variations and its magnetic field followed the same period. Using a slight variation of the Deutch (1958) model, Pyper identified four patches of iron-peak elements along the magnetic equator and one patch of rare earth elements near the negative magnetic pole. The spectral variations of α^2 CVn and other Ap stars can easily be explained by Pyper's model. Various other models have been proposed, *e.g.*, the method suggested by Falk & Wehlau (1974) makes use of line profiles for harmonic analysis instead of equivalent widths as was done by Pyper. Another method was developed by Khokhlova (1975) and Khokhlova & Rjabchikova (1975). In this method the line profiles are computed by putting spots of various elements over the surface of the star. This method has been extensively used by Khokhlova and her collaborators. More recently Vogt & Penrod (1983) have developed a technique called 'doppler imaging' on similar lines and used it successfully to map the surfaces of late-type spotted stars. Vogt, Penrod & Hatzes (1986) have improved the technique by incorporating the maximum entropy method for the construction of surface images of stars. They have applied this method to Ap stars as well (Hatzes, Penrod & Vogt 1986). All these methods of mapping the stellar surfaces using spectral line profiles have clearly indicated the presence of spots on these stars.

In order to describe the photometric variations in α^2 CVn and other Ap stars, Trasco (1972) developed a model that required high temperature magnetic regions.

Trasco suggested that at least three hot spots are required to produce the observed light variations of α^2 CVn.

Recently Böhm-Vitense & Van Dyk (1987) have come out with a new model for explaining the light curves of α^2 CVn. The model suggested by them is essentially an oblique rotator but the star is an oblate spheroid with the magnetic axis being the axis of symmetry. One might call it an oblique oblate rotator. They also assume a variable surface temperature. In this model the temperature at the magnetic poles is 1000 K less than that at the magnetic equator. As the star rotates, the combined effect of the variable surface temperature and the variable projected area of the star causes the observed light variation.

We describe below the spot models we have used for α^2 CVn to explain the spectroscopic and the photometric observations of Pyper (1969) and Molnar (1973). We make a comparison between the results obtained by our models and those obtained by Pyper. We further show that the results obtained by our spot models are in better agreement with the observations than the results obtained by the oblate spheroid model of Böhm-Vitense & Van Dyk (1987).

2. The spot model for spectroscopic variations

Pyper (1969) identified a concentration of iron-peak elements in four regions along the magnetic equator of the star. She called them group 2A, 2B, 2C, and 2D, respectively. She found rare earths to be concentrated near the negative magnetic pole; she called this group 1. Longitudes and latitudes of these groups, as determined by Pyper, are listed in Table 1, where group 1 is designated as 2E. Pyper did not specify sizes of these regions. But we can consider the size of the innermost contour of the constant equivalent width curve (Figs 12 and 13 in Pyper 1969) as the approximate size of each group. We have listed these sizes as well in Table 1. Using the spot parameters listed in Table 1, we tried to model the equivalent width variations observed by Pyper. This required computation of line profiles and measurement of their equivalent widths at all the observed phases. We divide the star into several thousand small areas—specifically, 20520 area elements. This is done by dividing the projected stellar disc into 57 annuli and 360 sectors of 1 degree. We use 57 intensity profiles in all from the centre to the limb of the star. The line profile from each area is Doppler shifted according to the line-of-sight velocity of that area element. Summation of all such profiles then provides the flux profile and its area provides the equivalent width. This is done at each observed phase. This scheme of division of stellar disc into area elements is the same as described by Gray (1982).

Table 1. Spot parameters obtained by Pyper (1969).

|	Spot 2A	Spot 2B	Spot 2C	Spot 2D	Spot 2E
Longitude	300	210	155	50	0
Latitude	10	−20	−25	20	−40
Radius*	20	22	15	15	25

Longitude, latitude, and radius are in degrees.
* see explanation in text.
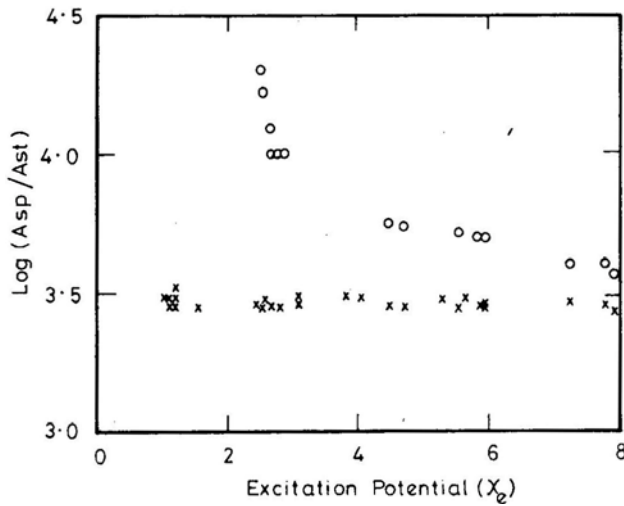
Figure 1. The spot-to-star abundance ratio is plotted against the excitation potential. The open circles refer to the case where spotted and unspotted regions are taken to be at the same temperature. The crosses are for the case where spot temperature is higher by 1000 K than the unspotted region.

In our first attempt, we used different elemental abundances for the spotted and unspotted regions, but no temperature difference between the two. This, however, did not provide us a satisfactory fit to the observations initially. But after a few trials with different abundances in spots, we arrived at a reasonably good match between the modelled equivalent width variations and the observed ones. But, here we encountered another problem. When we plotted the spot-to-star abundance ratio against the excitation potentials (χ_e) for various lines, we found that this ratio varied with χ_e. This is shown in Fig. 1 by open circles. We soon realized that our assumption of same temperature for the spotted and the unspotted regions was the cause of such behaviour of spot-to-star abundance ratio. The inverse correlation between abundance and excitation potential indicates that the higher levels have to be more populated, which means that the spots should have a higher temperature. A large abundance of elements in the spots will also increase the opacity and therefore the temperature in the spots should increase due to the backwarming. Both these reasonings made us to raise the spot temperature. After a few trials we settled for a spot temperature 1000 K higher than that of the unspotted region which was taken to be 12000 K. Once again the spot-to-star ratio was plotted against the excitation potential and was found to be reasonably constant for all the χ_e values. This is shown in Fig. 1 by crosses.

The equivalent width changes as the projected area of the spots changes due to rotation of the star. A value of $V \sin i = 23.0$ km s^{-1} was used in this model. We carried out these computations for all the lines that Pyper used in measuring the equivalent widths. Finally a mean curve was obtained for all the lines and normalized with respect to the maximum equivalent width computed. In Fig. 2 we have superimposed our model calculations on the observations of Pyper. We see that the spot model provides a good agreement with the observations. For group 2C our fit was not good at all, presumably because, according to Pyper (1969), at these phases her equivalent width
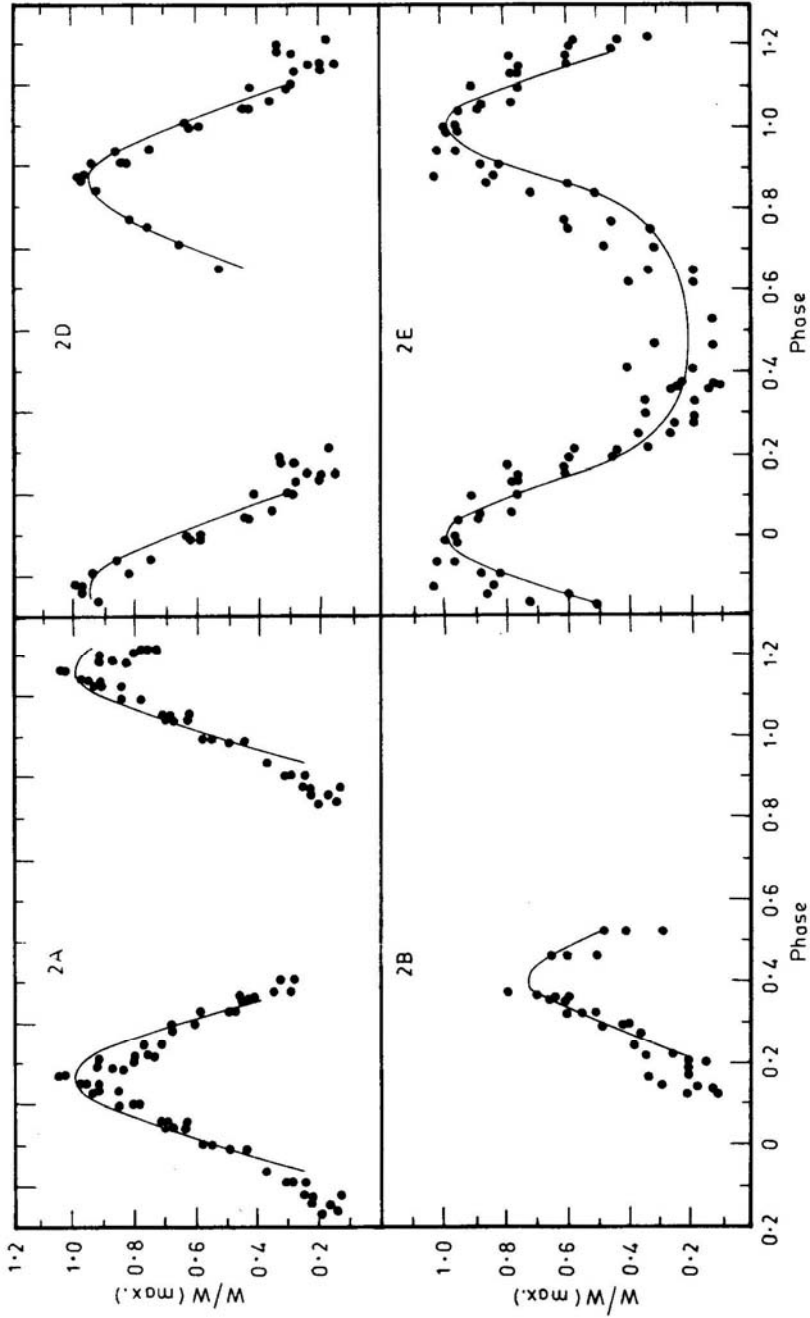
Figure 2. The top and bottom panels show the equivalent width variations observed by Pyper (1969). The solid line is the fit we obtained with our spot model.

measurements were of low accuracy. For this reason we have excluded the fit for group 2C from this figure.

In this model we consistently found a spot-to-star abundance ratio of 3×10^3 for iron peak elements (Fe, Ti, Cr) and 2×10^3 for rare earths (Eu, Gd). This means that if the unspotted region has a normal solar abundance then the spots will have a three orders of magnitude more of these elements. Such an abundance seems to be very high. Cohen (1970), by her LTE analysis of abundance determination, showed that the iron-peak elements are about two orders of magnitude more abundant in α^2 CVn. Her abundance determinations, however, refer to whole of the stellar surface, whereas our values are a ratio of abundances between the spot and the photosphere. A large spot-to-star abundance ratio, however, is not very uncommon. For HD 140160, a Sr-Ap star, an overabundance of Sr upto 10^3 was found in three spots by Khokhlova & Rjabchikova (1975). Like Cohen (1970) and Khokhlova & Rjabchikova (1975) our line profile calculations are also based on LTE approximation without taking into account the effect of magnetic field. Since atomic parameters, *e.g.*, gf values, for many lines are not known accurately, we take $gf = 1$ for all the lines while computing l_v. Thus, in that case

$$gfA_{\text{spot}}/gfA_{\text{star}} = A_{\text{spot}}/A_{\text{star}}.$$

Further we assume the microturbulence value of 2 km s^{-1} in spotted as well as in unspotted regions. We use Kurucz (1979) LTE model atmospheres for both the spotted and unspotted line computations. Because of these assumptions and approximations, we consider our derived values of spot-to-star abundance ratios as order of magnitude estimates only. For more accurate abundances a detailed abundance analysis, which takes into account the non-LTE effects and the effect of the presence of magnetic field, is called for. The assumptions made in our model were necessary to hold down the considerable computer time this model requires. We also notice that, even after all these approximations, a spot model can reliably reproduce the equivalent width variations observed in α^2CVn.

3. The spot model for photometric variations

The basic model is the same as that suggested by Budding (1977) and later by Poe & Eaton (1985) for late-type stars. We have made a small change in it to include a flux blocking parameter which is used in far ultraviolet region where the flux is known to be much more depressed in α^2 CVn than in a normal star of the same temperature. We have already seen in Section 2 that the spots are at higher temperature than the surrounding photosphere and have high concentration of iron-peak elements and rare earths. Therefore, we can assume that the far-ultraviolet flux-blocking takes place only in the spotted regions. Here spots are considered to be circular in shape and the star is a sphere of unit radius. The change in the light level due to the presence of the spot is given by

$$\Delta L = [\, F\,(T_{\text{star}}) - (1 - \beta)\, F\,(T_{\text{spot}})\,]\, \sigma_{\text{c}},$$

where $F\,(T_{\text{spot}})$ and $F\,(T_{\text{star}})$ are fluxes from the spot and surrounding photosphere at the temperatures T_{spot} and T_{star}, respectively, β is the flux-blocking parameter, and σ_{c} is

the limb-darkening-weighted projected area of the spot. It is given by

$$\sigma_c = 3/(3 - u) \{(1 - u)\,\sigma_0^0 + u\sigma_1^0\},$$

where u is the limb-darkening coefficient. The expressions for computing σ_0^0 and σ_1^0 are given by Budding (1977). Therefore, at a phase θ, the light from the star, normalized to unit value, becomes

$$L(\theta) = 1 - [F(T_{star}) - (1 - \beta)\,F(T_{spot})]\,\sigma_c$$

or
$$L(\theta) = 1 - [1 - (1 - \beta)\,F_{ratio}]\,\sigma_c,$$

where F_{ratio} is the spot-to-star flux ratio, $L(\theta)$ is then converted into magnitude as

$$m(\theta) = -2.5\,\log L + M_{ref},$$

where M_{ref} is the reference magnitude normally chosen to be at the star's brightest phase. We have further converted these magnitudes as

$$\Delta m\,(\theta) = m\,(\theta) - m(0),$$

where $m(0)$ is the magnitude at 0 phase. This enables us to compare our results with those obtained by Böhm-Vitense & Van Dyk (1987). The limb-darkening coefficients for $\lambda 2462$, $\lambda 2985$, $\lambda 3317$ and for U, B and V bandpasses are taken from Al-Naimy (1977) and are considered to be the same for the spots and the surrounding region. For $\lambda 1332$, $\lambda 1420$, and $\lambda 1554$ the limb darkening coefficients are not available, therefore for these wavelengths we use $u = 1$.

4. Computation of light curves

The above model was used for generating the theoretical far-ultraviolet and *UBV* light curves. These computed light curves are then compared with the observed ones given by Molnar (1973) and Pyper (1969). We fixed the temperature of the unspotted region at 12000 K, which is the same as the one used by Böhm-Vitense & Van Dyk for the equatorial region in their model. The inclination of star's rotation axis to the line of sight is taken to be 50 degrees. We computed several light curves for each bandpass using three, four, and five spots. In every case light curves with five spots provided minimum $(O - C)$'s. Later we fixed the number of spots as five. Longitudes and latitudes of spots were determined by trial and error. Some adjustments in area and temperature of spots had to be made, as these two quantities are strongly coupled. We adjusted the spot areas such that either the temperature or the spot-to-star flux ratio was the same at least in two bandpasses. In Fig. 3a we show our computed far-ultraviolet light curves superimposed on Molnar's observations. In Fig. 3b we show the computed light curves of Böhm-Vitense & Van Dyk (1987) that they obtained by oblate spheroid model. The oblate spheroid model light curves were read off from the best fit obtained by Böhm-Vitense & Van Dyk (Fig. 8 in their paper). The far ultraviolet observations of α^2 CVn by Molnar (1973) and later by Leckrone & Snijder (1979) show large flux deficiency in this region of the spectrum. Molnar (1973) attributes this large flux deficiency to the strong line blanketing by the rare earths. For below $\lambda 1600$ Å he suggests a second source of flux blocking which is a combination of continuous opacities and line blanketing from the iron-peak and rare-earth elements.

If these elements are concentrated in the spots, then the far-ultraviolet opacity will be larger for the spotted regions than for the unspotted ones. This implies that we will 'see' only top low-flux layers of spots, and deeper high-flux layers in the spot-free areas. This is where we have to make use of the flux-blocking parameter β in our model. For $\lambda 1332$, $\lambda 1420$, and $\lambda 1554$ we use $\beta = 0.7$, for $\lambda 2462$ and $\lambda 2985$ the value of β is 0.5 and 0.15, respectively. For $\lambda 3317$ and longward, *i.e.*, in *U*, *B*, and *V* bandpasses β is set equal to zero. These values roughly correspond to the fractional difference between Klinglesmith's (1971) hydrogen-blanketed model energy distribution and the observed energy distribution of α^2 CVn as shown in the Fig. 5 of Molnar (1973). In Table 2 we have listed the spot longitudes, latitudes and radii obtained in far-ultraviolet wavelength region. There was hardly any (or very little) change in the values of these quantities with wavelength.

On the longer-wavelength side the *U* and *B* spot temperatures (blackbody) agree well within 300 K. We get consistently a higher temperature for spots 1, 4 and 5 in the *V* bandpass. This could perhaps be due to our looking deeper in atmosphere in *V* band. One should notice that the variation in the *V* observations is almost twice as much as in *U* and *B*. In order to model this large *V* amplitude we were forced to use a higher spot-to-star flux ratio (thereby a higher spot temperature in *V* band compared to *U* and *B*). Another alternative could have been to reduce the star temperature or change
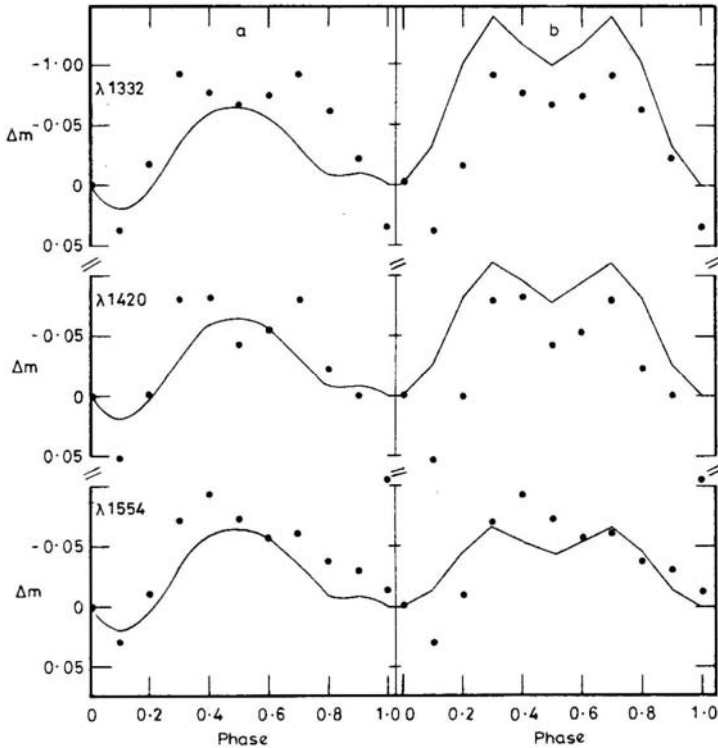
Figure 3. The calculated far-ultraviolet light curves (solid line) are superimposed on Molnar's (1973) observations (points): (a) our spot model; (b) oblate spheroid model of Böhm-Vitense & Van Dyk (1987).
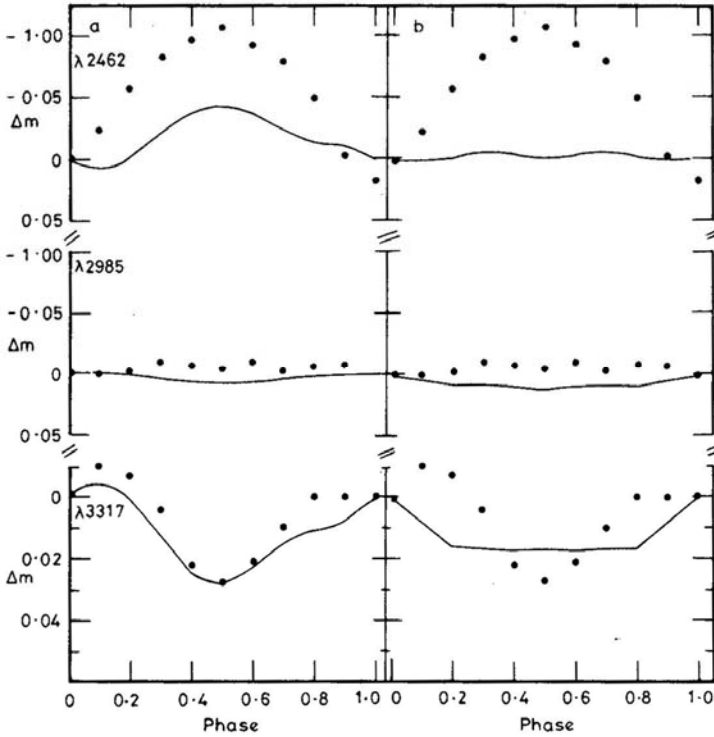
Figure 3. Continued.

Table 2. Spot parameters obtained by our spot model in far ultraviolet.

	Spot 1	Spot 2	Spot 3	Spot 4	Spot 5
Longitude	300	225	140	60	330
Latitude	10	−30	−30	20	−35
Radius	16	10	10	15	30

Longitude, latitude, and radius are in degrees.

the spot area drastically in this bandpass. None of these options seems to be reasonable when spot parameters derived from the other two bandpasses agree so well. We have listed these spot parameters for all five spots in Table 3. In Fig. 4(a) we have plotted our computed *UBV* light curves on top of Pyper's observations. In Fig. 4(b) light curves obtained by oblate spheroid model are plotted on Pyper's observations. Once again the oblate spheroid model light curves were read off from the best fit obtained by Böhm-Vitense & Van Dyk (1987; Fig. 10). It is clearly evident from Figs 2, 3 and 4 that the hot-spot model gives a far better fit to the observed data than the one suggested by Böhm-Vitense & Van Dyk.

If one looks at the observed light curves carefully, one notices an initial increase in *U* and *B* with a peak at 0.1 phase. This initial increase could not be explained by the oblate-spheroid model. But our spot model calculations do reproduce this peak in

Table 3. Spot parameters obtained by our spot model.

	Spot 1			Spot 2			Spot 3			Spot 4			Spot 5		
	V	B	U	V	B	U	V	B	U	V	B	U	V	B	U
Longitude	320	300	300	250	250	250	155	145	145	40	50	60	350	350	330
Latitude	8	10	10	−30	−30	−28	−30	−30	−28	20	20	20	−40	−40	−35
Radius	24	20	16	8	14	12	8	8	12	18	15	15	25	25	30
F_{sp}/F_{st}	1.30	1.26	1.27	1.08	1.20	1.23	1.08	1.20	1.23	1.30	1.26	1.24	1.30	1.26	1.23
T(spot)	13409	13024	12888	12386	12795	12762	12386	12795	12762	13409	13024	12793	13409	13024	12762

Longitude, latitude, and radius are in degrees. F_{sp}/F_{st} is spot-to-star flux ratio (F_{ratio}).
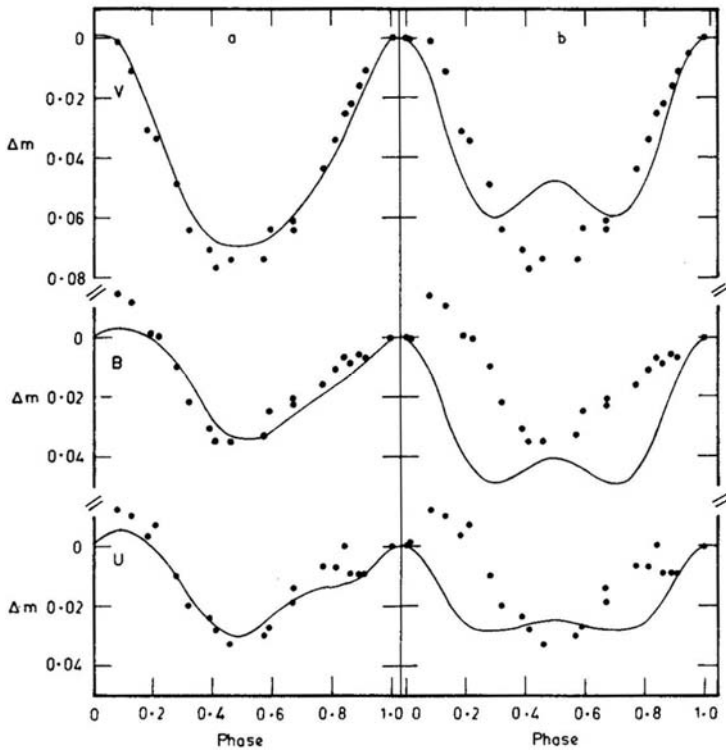
Figure 4. The model *VBU* light curves (solid line) are superimposed on Pyper's (1969) observations (points): (a) our spot model; (b) oblate spheroid model of Böhm-Vitense & Van Dyk (1987).

light satisfactorily. An exactly reverse behaviour is seen in the far-ultraviolet observations of Molnar (1973). Our model is again able to reproduce it. We find that the spot 5, which happens to be close to negative magnetic pole, is responsible for this.

A comparison between the parameters listed in Tables 1, 2 and 3 shows that there is a close agreement between the spot positions obtained by us and those given by Pyper; spot sizes, however, do not agree so well. This is because we have taken the innermost equivalent width contour as the spot size; the actual spot size and shape may differ. But the overall agreement is reasonably good.

5. Summary and conclusion

With the models described above we are able to show that, for α^2 CVn, a model consisting of five hot spots (300 to 800 K hotter than the surrounding atmosphere) can reproduce observed light curves better than the oblate-spheroid model which has a variable surface temperature as well as a variable apparent radius of the star. We also show that a spot model is needed to explain the observed equivalent-width variations. The spot positions obtained by us in our photometric model agree well with those obtained spectroscopically by Pyper (1969).

The Ap stars have fairly stable atmospheres. Such stable atmospheres are necessary if diffusion of elements is to work (Michaud 1970). However, with hot spots it becomes difficult to explain how can such hot regions survive for a long time in a cooler atmosphere. Perhaps some mechanism is at work so that there is a rapid loss of heat from these hot regions. Trasco (1972) has shown that, for magnetic stars, an equilibrium condition will exist when the temperature in the magnetic region is higher than the non-magnetic region. We believe that the spots on α^2 CVn are associated with such fields and therefore are at higher temperature than the nonmagnetic regions.

Acknowledgement

References

Al-Naimy, H. M. 1977, *Astrophys. Sp. Sc.*, **53,** 181.

Böhm-Vitense, E., Van Dyk, S. D. 1987, *Astr. J.*, **93,** 1527.

Budding, E. 1977, *Astrophys. Sp. Sc.*, **48,** 207.

Cohen, J. G. 1970, *Astrophys. J.*, **159,** 473.

Deutch, A. J. 1958, in *IAU Symp.* 6: *Electromagnetic Phenomena in Cosmical Physics*, Ed. B. Lehnert, University Press, Cambridge, p. 209.

Falk, A. E., Wehlau, W. H. 1974, *Astrophys. J.*, **192,** 409.

Gray, D. F. 1982, *Astrophys. J.*, **258,** 201.

Guthnick, P., Prager, R. 1914, *Veröff. Sternw.* Berlin-Babelsberg, **1,** 38.

Hatzes, A. P., Penrod, G. D., Vogt, S. S. 1986, *Bull. Am. astr. Soc.* **18,** No. 2, p. 668.

Khokhlova, V. L. 1975, *Astr. Zh.* **52,** 950.

Khokhlova, V. L., Rjabchikova, T. A. 1975, *Astrophys. Sp. Sc.*, **34,** 403.

Klinglesmith, D. A. 1971, NASA SP - 3065.

Kurucz, R. L. 1979, *Astrophys. J. Suppl.*, **40,** 1.

Leckrone, D. S., Snijders, M. A. J. 1979, *Astrophys. J. Suppl.*, **39,** 549.

Michaud, G. 1972, *Astrophys. J.*, **160,** 641.

Molnar, M. R. 1973, *Astrophys. J.*, **179,** 527.

Poe, C. H., Eaton, J. A. 1985, *Astrophys. J.*, **289,** 644.

Pyper, D. M. 1969, *Astrophys. J. Suppl.*, **18,** 347.

Trasco, J. D. 1972, *Astrophys. J.*, **171,** 569.

Vogt, S. S., Penrod, G. D. 1983, *Publ. astr. Soc. Pacific*, **95,** 565.

Vogt, S. S., Penrod, G. D., Hatzes, A. P. 1986, *Preprint*.